

CP VIOLATING PHASES IN SUSY GUT MODELS*

E. ACCOMANDO, R. ARNOWITT AND B. DUTTA

Center For Theoretical Physics, Department of Physics, Texas A&M University, College Station TX 77843-4242

Supersymmetric CP violating phases are examined within the framework of gravity mediated supergravity grand unified models with R parity invariance for models with a light ($\lesssim 1$ TeV) particle spectrum. In the minimal model, the nearness of the t quark Landau pole naturally suppresses the t-quark cubic soft breaking parameter at the electroweak scale allowing the electron and neutron experimental electric dipole moment (EDM) constraints to be satisfied with a large GUT scale phase. However, the EDM constraints require that θ_B , the quadratic soft breaking parameter phase be small at the electroweak scale unless $\tan\beta \lesssim 3$, which then implies that at the GUT scale this phase must be large and highly fine tuned to satisfy radiative breaking of $SU(2) \times U(1)$. Similar results hold for non minimal models, and a possible GUT model is discussed where all GUT scale CP violating phases are naturally small (i.e. $O(10^{-2})$). An interesting D-brane model is examined which enhances the size of the phases over much of the parameter space at the electroweak sector for $\tan\beta \lesssim 5$, but still possesses the fine tuning problem at the GUT scale.

1 Introduction

The Standard Model (SM) of strong and electroweak interactions is a remarkably rigid theory of quark and lepton interactions. Thus the gauge invariance guarantees baryon and lepton number invariance and forbids bare mass terms. In order to generate quark and lepton masses, one introduces Higgs Yukawa couplings, and the spontaneous breaking of $SU(2) \times U(1)$ simultaneously generates the necessary masses, both in the gauge boson and fermionic sectors. For the three generations that have been observed, the Yukawa matrices allow for only one CP violating phase in the CKM matrix, which is consistent with the observed CP violation in the K meson system (and these ideas will be tested for B mesons with future data from B factories and high energy accelerators.). Further this phase gives only a very small contribution to the electron and neutron electric dipole moments (EDMs), d_e and d_n . In supersymmetry (SUSY) extensions of the SM, things are more complicated. One generally imposes R-parity invariance to suppress too rapid proton decay, and there is now an array of possible new CP violating phases arising from the SUSY soft breaking masses which generally produce large contributions to d_n and d_e . The current experimental EDM bounds are for d_n ¹ and d_e ²:

$$(d_n)_{exp} < 6.3 \times 10^{-26} ecm; 90\% C.L. \quad (1)$$

$$(d_e)_{exp} < 4.3 \times 10^{-27} ecm; 95\% C.L. \quad (2)$$

In the past, two suggestions have been made to accomodate these bounds: (i) one can assume the CP violating phases are small i.e. $\phi = O(10^{-2})^3$ and/or (ii) the SUSY mass spectrum is heavy i.e. squark (\tilde{q}), slepton (\tilde{l}) and gluino (\tilde{g}) masses are

*BASED ON TALK AT SSS-99, SEOUL, KOREA, JUNE, 1999

$\gtrsim O(1\text{TeV})$ ⁴. The first hypothesis would appear to require a significant amount of fine tuning (though see sec. 4 below), while the second would place the SUSY spectrum beyond the reach of even the LHC and regenerate the gauge hierarchy problem. Recently, it has been observed that a third option is possible, i.e. that cancellations can naturally occur in the total EDM amplitude (e.g. between neutralino and chargino contributions) allowing one to satisfy Eqs. (1,2) with relatively large phases (i.e. $O(10^{-1})$) and a light SUSY spectrum $< O(1\text{TeV})$ ⁵., and there has been considerable investigation of this possibility ^{5,6,7,8,9,10,11,13,14}. The work presented here is given in Ref^{15,16}.

We consider here these possibilities within the framework of supergravity (SUGRA) grand unified models (GUTs) with gravity mediated SUSY breaking and R-parity invariance ¹⁷. For other work within this framework see ^{5,6,8,9,12,13}. Here the low energy predictions of the model are determined from the GUT scale M_G parameters by running the renormalization group equation from M_G to the electroweak scale M_{EW} . Such a theory is considerably more constrained than the purely phenomenological low energy MSSM model. Thus (1) there are considerable constraints arising from the GUT group symmetry, (2) CP violating phases and SUSY parameters that are arbitrary in the MSSM get correlated by the RGE, (3) radiative breaking of $SU(2) \times U(1)$ at M_{EW} puts additional constraints on the CP violating phases and SUSY parameters.

In models of this type, what is natural or unnatural is a property of the theory at M_G rather than M_{EW} . Thus we find that some phases that are naturally large at M_G get suppressed at M_{EW} leading, hence, to a “naturally” small phase there. However, unless $\tan\beta \lesssim 3$ (assuming SUSY masses are not large) one phase at M_{EW} is quite small, and the RGE then implies that it is both large and highly fine tuned at M_G . In addition, while there is considerable theoretical uncertainty in the calculation of d_n , the combined constraints of d_n and d_e of Eqs. (1,2) put significant additional constraints on the allowed SUSY parameter space.

The above results hold for both for the minimal mSUGRA model and generally for models with nonuniversal soft breaking. We will also discuss one very interesting D-brane model with nonuniversal soft breaking ¹².

2 Electric Dipole Moments For mSUGRA Models

We consider first the simplest case where there is universal SUSY soft breaking parameters at M_G . The theory then depends on five parameters: m_0 (the universal squark and slepton mass at M_G), $m_{1/2}$ (the universal gaugino mass at M_G), A_0 (the cubic soft breaking parameter at M_G), B_0 (the quadratic soft breaking parameter at M_G) and μ_0 (the Higgs mixing parameter at M_G in the superpotential). Of these the last four can be complex. However, one may make a phase rotation to make $m_{1/2}$ real, leaving A_0 , B_0 and μ_0 complex at M_G :

$$A_0 = |A_0|e^{i\alpha_{0A}}; B_0 = |B_0|e^{i\theta_{0B}}; \mu_0 = |\mu_0|e^{i\theta_{0\mu}}. \quad (3)$$

The RGE determines the low energy parameters in terms of the M_G parameters. Thus there results a different A parameter at M_{EW} (which we take to be m_t), for

each squark and slepton e.g. $A_t, A_b, A_\tau, A_u, A_d, A_e$ and we label these by

$$A_t = |A_t|e^{i\alpha_t}; B = |B|e^{i\theta_B}; \mu = |\mu|e^{i\theta_\mu}; etc \quad (4)$$

(Note that to one loop order $\theta_{0\mu} = \theta_\mu$.) The $SU(3)_C$, $SU(2)_L$ and $U(1)_Y$ gaugino masses are labeled \tilde{m}_3 , \tilde{m}_2 and \tilde{m}_1 and remain real at one loop..

The effective Lagrangian for d_f , the EDM of fermion of type f (quark or lepton) is

$$L_f = -\frac{i}{2}d_f \bar{f} \sigma_{\mu\nu} \gamma^5 f F^{\mu\nu}. \quad (5)$$

The basic diagrams for d_f that contribute to L_f at M_{EW} are given in Fig.1.

The calculation of the neutron EDM contains a number of uncertainties due to QCD effects. To relate d_n to the quark EDMs d_u and d_d , we use the non relativistic quark model relation

$$d_n = \frac{1}{3}(4d_d - d_u) \quad (6)$$

. In addition to Eq.5, one must take into account the gluonic operators L^C and L^G given by

$$L^C = -\frac{i}{2}d^C \bar{q} \sigma_{\mu\nu} \gamma^5 T^a q G_a^{\mu\nu} \quad (7)$$

$$L^G = -\frac{1}{3}d^G f_{abc} G_{a\mu\alpha} G_{b\nu}^\alpha \tilde{G}_c^{\mu\nu} \quad (8)$$

where $\tilde{G}_c^{\mu\nu} = \frac{1}{2}\epsilon^{\mu\nu\alpha\beta} G_{c\alpha\beta}$ ($\epsilon^{0123} = 1$), $T^a = \frac{1}{2}\lambda^a$ (λ^a are the $SU(3)$ Gell-Mann matrices), $G_a^{\mu\nu}$ are the $SU(3)$ field strengths and f_{abc} are the $SU(3)$ structure constants. Contributions to L^C arise from Fig.1 with γ replaced by g and the two loop Barr-Zee type diagrams of Fig.2¹⁸. Contributions to L^G come from the two loop Weinberg type diagram of Fig.3¹⁹. One must use the QCD RGE factors η^{ED} , η^G , η^C to evolve the results from M_{EW} down to 1 GeV²⁰ and we use the naive dimensional analysis²¹ to relate d^C and d^G to d_f . In calculating d_q , one needs to know the quark masses m_u and m_d . While the mass ratios are fairly well known²²,

$$\frac{m_u}{m_d} = 0.553 \pm 0.043; \quad \frac{m_s}{m_d} = 18.9 \pm 0.8 \quad (9)$$

m_s is in considerable doubt, i.e. QCD sum rules give $m_s = (175 \pm 25)$ MeV and lattice gauge theory gives $m_s(2GeV) = (100 \pm 20 \pm 10)$ MeV in the quenched lattice calculation. (Lowering the scale to 1 GeV will increase m_s , but unquenching will reduce it).

We see in general that there are significant uncertainties in calculating d_n (perhaps a factor of 2-3). In the following we will assume $m_s = 150$ GeV ($m_d \cong 8$ MeV, $m_u \cong 4.4$ MeV), but we will exhibit below the sensitivity of d_n to the uncertainty in m_s .

$SU(2) \times U(1)$ breaking at M_{EW} gives rise to Higgs VEVs which in general may be complex:

$$< H_{1,2} > = v_{1,2} e^{i\epsilon_{1,2}}; \quad v_{1,2} \equiv | < H_{1,2} > | \quad (10)$$

and we define $\tan\beta = v_2/v_1$. One may chose matter phases so that the chargino mass matrix takes the form:

$$M_{\chi^\pm} = \begin{pmatrix} \tilde{m}_2 & \sqrt{2}M_W \sin\beta \\ \sqrt{2}M_W \cos\beta & -|\mu|e^{i\theta} \end{pmatrix} \quad (11)$$

where $\theta = \epsilon_1 + \epsilon_2 + \theta_\mu$. The neutralino mass matrix is:

$$M_{\chi^0} = \begin{pmatrix} \tilde{m}_1 & 0 & a & b \\ 0 & \tilde{m}_2 & c & d \\ a & c & 0 & |\mu|e^{i\theta} \\ b & d & |\mu|e^{i\theta} & 0 \end{pmatrix} \quad (12)$$

where $a = -M_Z \sin\theta_W \cos\beta$, $b = M_Z \sin\theta_W \sin\beta$, $c = -\cot\theta_W a$, $d = -\cot\theta_W b$. The squark mass matrices is

$$M_{\tilde{q}}^2 = \begin{pmatrix} m_{qL}^2 & e^{-i\alpha_q} m_q (|A_q| + |\mu| R_q e^{i(\theta+\alpha_q)}) \\ e^{i\alpha_q} m_q (|A_q| + |\mu| R_q e^{-i(\theta+\alpha_q)}) & m_{qR}^2 \end{pmatrix} \quad (13)$$

where m_q , e_q are the quark mass and charge,

$$m_{qL}^2 = m_Q^2 + m_q^2 + (1/2 - e_q \sin^2\theta_W) M_Z^2 \cos 2\beta \quad (14)$$

$$m_{qR}^2 = m_U^2 + m_q^2 + e_q \sin^2\theta_W M_Z^2 \cos 2\beta \quad (15)$$

where $R_q = \cot\beta(\tan\beta)$ for u(d) quarks and m_Q^2 , m_U^2 are given in ²³. (A Similar result holds for the sleptons).

The Higgs VEVs are determined by minimizing the effective potential

$$V_{eff} = m_1^2 v_1^2 + m_2^2 v_2^2 + 2|B\mu| \cos(\theta + \theta_B) v_1 v_2 + \frac{g_2^2}{8} (v_1^2 - v_2^2)^2 + \frac{g'^2}{8} (v_2^2 - v_1^2)^2 + V_1 \quad (16)$$

where V_1 is the one loop contribution

$$V_1 = \frac{1}{64\pi^2} \sum_a C_a (-1)^{2j_a} (2j_a + 1) m_a^4 \left(\ln \frac{m_a^2}{Q^2} - \frac{3}{2} \right). \quad (17)$$

Here C_a , j_a and m_a are the color factor, spin and mass of particle a and $Q = m_t$ is the electroweak scale. In the following we include the full third generation of states in V_1 (t, b τ) so that we can consider large $\tan\beta$. The minimization of the tree contribution gives

$$\theta = \pi - \theta_B. \quad (18)$$

From Eq.(13), the mass eigenvalues entering into Eq.(17) depends only on $\theta + \alpha_q$ and $\theta + \alpha_l$, so that minimizing the tree plus loop V_{eff} gives

$$\theta = \pi - \theta_B + f_1(\pi - \theta_B + \alpha_q, \pi - \theta_B + \alpha_l) \quad (19)$$

where f_1 is the one loop correction. As we will see, this correction can become significant for large $\tan\beta$. However, as we will see below, it can make important contributions for large $\tan\beta$ since the EDMs are sensitive to θ_B .

A convenient way of characterizing how close the theory is in accord with the EDMs is given by the parameter K :

$$K = \log_{10} \left| \frac{d_f}{(d_f)_{exp}} \right| \quad (20)$$

where $(d_f)_{exp}$ is the current experimental bound. Thus $K \leq 0$ is required for the theory to be in accord with experiment. An example of K as a function of m_0 is given in Fig.4. One sees that the width of the allowed $K \leq 0$ region decreases as $\tan\beta$ increases. Eventually, for very large m_0 , one would obtain $K < 0$ even for large $\tan\beta$ (the heavy SUSY spectrum option). For $m_0 < 1$ TeV, we see that the region $K \leq 0$ moves to lower m_0 . The reason for this is that the chargino diagram increases more rapidly with $\tan\beta$ than the neutralino diagram, and in order to maintain the cancelation between them to satisfy $K \leq 0$ one must decrease m_0 to enhance the neutralino diagram relative to the chargino. The above discussion shows that the cancelations needed to achieve $K \leq 0$ are relatively delicate, and would become increasingly so if e.g. the experimental bounds are reduced by a factor of 10 ($K \leq -1$).

To understand what parameters control cancelations, one may look at the RGE which relate the GUT scale parameters to electroweak scale parameters. The one loop RGE must be solved numerically. However, for small or intermediate $\tan\beta$ (and also in the SO(10) limit) analytic solutions are available which allow one to see analytically what is happening. Thus for low $\tan\beta$ one finds for A_t the result

$$A_t = D_0 A_0 + \Phi_A m_{1/2} \quad (21)$$

where Φ_A is real and $O(1)$ and $D_0 \cong 1 - (m_t/200 \sin\beta)^2$. Thus D_0 is small i.e. $D_0 \lesssim 0.2$. The imaginary part of Eq.(21) gives:

$$|A_t| \sin\alpha_t = |A_0| D_0 \sin\alpha_{0A} \quad (22)$$

Thus because D_0 is small (the nearness of the t-quark Landau pole) the phase α_t is suppressed relative to α_{0A} . Thus even if $\alpha_{0A} = \pi/2$, α_t is sufficiently reduced at the electroweak scale so that the EDM constraints may be satisfied. Hence in mSUGRA, no fine tuning of α_{0A} is necessary.

The situation, however, is more difficult for the θ_B phase. For low and intermediate $\tan\beta$ (and similar results hold for large $\tan\beta$ in the SO(10) limit) the RGE solution is

$$B = B_0 - \frac{1}{2}(1 - D_0)A_0 + \Phi_B m_{1/2} \quad (23)$$

where Φ_B =real and $O(1)$. The imaginary and real parts give

$$|B| \sin\theta_B = |B_0| \sin\theta_{0B} - \frac{1}{2}(1 - D_0)|A_0| \sin\alpha_{0A} \quad (24)$$

$$|B| \cos\theta_B = |B_0| \cos\theta_{0B} - \frac{1}{2}(1 - D_0)|A_0| \cos\alpha_{0A} + \Phi_B m_{1/2}. \quad (25)$$

These may be viewed as equations to determine $|B|$ and θ_B in terms of the GUT scale parameters. Alternatively, one may impose phenomenological constraints at

the electroweak scale to see what GUT scale parameters will satisfy them. Two such constraints are the experimental EDM bounds, and the requirement of radiative breaking of $SU(2) \times U(1)$ at the electroweak scale. The latter implies that

$$|B| = \frac{1}{2} \sin 2\beta \frac{m_3^2}{|\mu|} \quad (26)$$

where $m_3^2 = 2|\mu|^2 + m_{H_1}^2 + m_{H_2}^2 + 1\text{loop}$, where $m_{H_i}^2$ are the Higgs running masses.

The EDM constraints, generally require that θ_B be small i.e. $\theta_B \lesssim 0.2$. Since $\frac{1}{2} \sin 2\beta \simeq (1/\tan\beta)$, the r.h.s. of Eq.(26) is a decreasing function of $\tan\beta$, and hence it determines $|B|$ to be small unless $\tan\beta \lesssim 3$. Returning to Eq.(24), one sees that the l.h.s. is thus quite small and so θ_{0B} is scaled by α_{0A} . Hence if α_{0A} is not fine tuned to be small, we find that the GUT scale θ_{0B} must be large i.e. $O(1)$. (This is indeed confirmed by detailed numerical calculations.) Consider now the situation where one fixes A_0 at M_G , and let $\Delta\theta_B$ be the allowed range of θ_B satisfying the EDM constraints. One has $\Delta\theta_B \lesssim 0.2$ and in general smaller. From Eq. (24) we see the corresponding allowed range at M_G is

$$\Delta\theta_{0B} \cong \frac{|B|}{|B_0|} \Delta\theta_B \ll \Delta\theta_B \quad (27)$$

and by $SU(2) \times U(1)$ breaking constraint Eq. (26) one will have $\Delta\theta_{0B} \ll \Delta\theta_B$ unless $\tan\beta \lesssim 3$. Fig.5, where the value of θ_{0B} obeying the EDM constraint is plotted as a function of $m_{1/2}$ for $|A_0| = 300$ GeV and $\alpha_{0A} = \pi/2$ illustrates this effect. One sees that indeed θ_{0B} is large, and that even for $\tan\beta=3$, the allowed range of $\Delta\theta_{0B}$ satisfying the d_e constraint for $m_{1/2} \lesssim 350$ GeV ($m_{\tilde{g}} \lesssim 1$ TeV) is quite small. For $\tan\beta=10$, $\Delta\theta_{0B}$ is very small. (Note that the LEP bound on the Higgs mass already requires $\tan\beta \geq 2$.)

We see that the combined requirements of radiative electroweak breaking and the experimental EDM constraints lead to a serious fine tuning problem at the GUT scale: θ_{0B} is large and must be tightly fine tuned unless $\tan\beta$ is close to its minimum value $\tan\beta=2$ (unless SUSY masses are large, e.g. $\gtrsim 1$ TeV, and/ or all phases are small, e.g. $O(10^{-2})$.)

We discussed above the existence of uncertainties in calculating of the neutron EDM. We exhibit here the effect of the uncertainty in m_s in Eq.(9). Fig.6 plots $K=0$ contours corresponding to $m_d(1 \text{ GeV})=5, 8$ and 12 MeV for $\tan\beta=3$, $|A_0| = 300$ GeV and $\alpha_{0A} = \pi/2$. These values of m_d correspond to $m_s \cong 95, 151$ and 227 MeV respectively. (Current lattice calculations favor the lowest value.) We see that d_n is quite sensitive to m_d , the constraint being significantly less severe for the lower quark masses. In Fig.5 and subsequent figures, we have chosen the central value of $m_d=8$ MeV.

We also have mentioned above that the loop corrections in Eq. (19) can be significant for large $\tan\beta$. This is because f_1 which grows with $\tan\beta$, represents an effective shift in θ_B , and the EDM constraints require θ_B to be small. One can see this effect of f_1 in Fig. 7 for $\tan\beta=20$, where we have set $\theta_B = 0$ so that in this example f_1 is the total “effective” θ_B in Eq. (19). For large $m_{1/2}$, the shape of the curves resemble those of Fig.6. However for $175 \text{ GeV} \lesssim m_{1/2} \lesssim 400 \text{ GeV}$,

the f_1 contribution gives rise to cancelation in the EDM amplitudes to significantly reduce the excluded regions showing that the loop contributions are important for large $\tan\beta$. Note that the effect persists even for $K = -0.5$.

3 D-Brane Models

In SUGRA models, nonuniversal soft breaking can arise if the hidden sector fields in the Kahler potential which give rise to SUSY breaking do not couple universally to the physical sector fields. In this case nonuniversal squark, slepton and Higgs masses can be generated at M_G , as well as nonuniversal A parameters. For simple GUT groups, however, it is difficult to generate more than small nonuniversality in the gaugino masses at M_G . Models of this type behave qualitatively similar to the mSUGRA model discussed in Sec.II above i.e. no serious fine tuning is needed for α_{0A} , but θ_{0B} is generally large and highly fine tuned unless $\tan\beta \lesssim 3$.

We consider in this section a class of models based on Type IIB orientifolds where the existence of open string sectors imply the presence of Dp -branes, manifolds of $p+1$ dimensions in the full $D=10$ space of which 6 dimensions are compactified e.g. on a six torus T^6 . (For a general discussion of this class of models see ²⁴). Models of this type can contain 9 branes (the full 10 dimensional space) plus 5_i -branes, $i=1, 2, 3$ (6 dimensional space with two compact dimensions) or in the T-dual representation, 3 branes plus 7_i branes, $i=1, 2, 3$. Associated with a set of n coincident branes is a gauge group $U(n)$.

One can clearly embed the Standard model gauge group in a number of ways in such models. Recently, an interesting model has been proposed based on 9-branes and 5-branes ¹². In this model, $SU(3)_C \times U(1)_Y$ is associated with one set of 5-branes, i.e. 5_1 , and $SU(2)_L$ is associated with a second intersecting set 5_2 . Strings starting on 5_2 and ending on 5_1 have massless modes carrying the joint quantum numbers of the two branes i.e. the SM quark, lepton and Higgs doublets. Strings beginning and ending on 5_1 have massless modes carrying $SU(3)_C \times U(1)_Y$ quantum numbers i.e. the SM quark and lepton singlets. We assume all other possible fields at the compactification scale M_c are superheavy and can be ignored to first approximation, as far as the low energy predictions of the model are concerned. For models of this type $M_c = M_G$, while the string scale M_{str} , is given by $M_{str} = (\alpha_G M_c M_{Planck} / \sqrt{2})^{1/2} \cong 8 \times 10^{16}$ GeV (for $\alpha_G \cong 1/24$). Thus below M_G , the gauge interactions are the usual $D=4$ theory.

The gauge kinetic functions for 9 branes and 5_i -branes are given by ^{24,25} $f_9 = S$ and $f_{5_i} = T_i$ where S is the dilaton and T_i are moduli. The origin of SUSY breaking is not yet understood in string theory. It may be parametrized, however, by VEV growth of S and T_i . Further, in string theory, CP violation must also occur as a spontaneous breaking and it is natural to associate these two spontaneous breakings by assuming that the F-components grow complex VEVs which are parametrized by ^{24,26,27}

$$\begin{aligned} F^S &= 2\sqrt{3} \langle \text{Re}S \rangle \sin\theta_b e^{i\alpha_s} m_{3/2} \\ F^{T_i} &= 2\sqrt{3} \langle \text{Re}T_i \rangle \cos\theta_b \Theta_i e^{i\alpha_i} m_{3/2} \end{aligned} \quad (28)$$

where θ_b, Θ_i are Goldstino angles ($\sum \Theta_i^2 = 1$) and $m_{3/2}$ is the gravitino mass. In the

following we assume $\Theta_3 = 0$, $\langle \text{Re}T_i \rangle$ are equal (to guarantee grand unification at M_G), and $\langle \text{Im}T_i \rangle = 0$ (so that the spontaneous breaking does not grow a θ -QCD type term).

The above model then leads to the following soft breaking masses at M_G :

$$\tilde{m}_1 = \sqrt{3}\cos\theta_b\Theta_1e^{-i\alpha_1}m_{3/2} = \tilde{m}_3 = -A_0 \quad (29)$$

$$\tilde{m}_2 = \sqrt{3}\cos\theta_b\Theta_2e^{-i\alpha_2}m_{3/2} \quad (30)$$

and

$$m_{5_15_2}^2 = (1 - \frac{3}{2}\sin^2\theta_b)m_{3/2}^2 \quad (31)$$

$$m_{5_1}^2 = (1 - 3\sin^2\theta_b)m_{3/2}^2 \quad (32)$$

where $m_{5_15_2}^2$ are the soft breaking masses for q_L , l_L , $H_{1,2}$ and $m_{5_1}^2$ are for u_R , d_R and e_R . The B_0 and μ_0 parameters are not determined by the above considerations and are model independent. We therefore parametrize them phenomenologically by

$$B_0 = |B_0|e^{i\theta_{0B}}; \mu_0 = |\mu_0|e^{i\theta_{0\mu}}. \quad (33)$$

We can also chose phases such that $\alpha_2 = 0$.

We see that the D-brane model give rise to a soft breaking pattern uniquely different from what is seen in SUGRA GUT models. Thus it would be difficult to find a GUT group breaking where $\tilde{m}_1 = \tilde{m}_3 \neq \tilde{m}_2$ and and similarly the above pattern of sfermion and Higgs soft masses. Brane models can achieve the above pattern since they have the freedom of associating different parts of the SM gauge group with different branes. In particular, the fact that the \tilde{m}_1 and \tilde{m}_3 phases are equal causes cancelation between the gluino and neutralino EDM diagrams, and considerably aids in satisfying the EDM constraints. Fig.8 exhibits this phenomena where K is plotted as a function of θ_B for d_e for $\tan\beta=2$ (solid), 5 (dashed), 10 (dotted) with phases $\phi_1 = \phi_3 = \pi + \alpha_{0A} = -1.25\pi$ and $m_{3/2} = 150$ GeV, $\theta_b = 0.2$, $\Theta_1=0.85$. One sees that θ_B can be quite large and still satisfy the EDM bound $K \leq 0$, i.e. $\theta_B \simeq 0.4$ for $\tan\beta=2$ and $\theta_B \simeq 0.25$ even for $\tan\beta=10$. If one reduces the gaugino phases, e.g. to $\alpha_1 = \alpha_3 = -1.1\pi$, one finds $\theta_B < 0.2$ showing that the enhanced values of θ_B are indeed due to the cancellations allowed by the gaugino phases.

While θ_B can be relatively large at the electroweak scale, one finds as in the mSUGRA models, θ_{0B} at the GUT scale is large (when $\alpha_1 = \alpha_3 = \pi + \alpha_{0A}$ is large) but must be fine tuned, i.e. the allowed range $\Delta\theta_{0B}$ is small unless $\tan\beta$ is small. This is illustrated in Fig.9 where $\Delta\theta_{0B}$ is plotted as a function of $\tan\beta$. For these parameters ($\alpha_{0A} = -\pi/4$) there is already a 1 % finetuning in θ_{0B} at $\tan\beta=5$, with increased fine tuning required for higher $\tan\beta$. Thus this class of D-brane models does not resolve the fine tuning problem.

While as discussed in Sec.2 there are uncertainties in the calculation of the neutron EDM, it is of interest to see what parts of the parameter space remains if one requires that the experimental EDM constraint is satisfied simultaneously for d_e and d_n . (We assume here the validity of the calculations of d_n described in sec.2) An example of this is shown in Fig.10 where the allowed regions for d_e and d_n are shown for $\phi_1 = \phi_3 = \pi - \alpha_{0A} = -1.90\pi$ for different $\tan\beta$. One sees that the overlap

where the d_e and d_n EDM constraints are simultaneously satisfied disappears for $\tan\beta > 5$ for these parameters. Note also that while d_n can tolerate larger θ_B , to have both EDM constraints satisfied requires $\theta_B \lesssim 0.15$ in this example. In general, the overlap region broadens in Θ_1 the closer $\phi_1 = \phi_3$ is to -2π (i.e. real $\tilde{m}_1 = \tilde{m}_3$), but the allowed θ_B then becomes smaller (since the amount of neutralino-gluino cancelation is reduced).

4 Models with small phases

Both the SUGRA and D-brane models possess a serious fine tuning problem at M_G in θ_{0B} when phases are large unless $\tan\beta$ is small. For models of this type “naturalness” is to be defined at M_G , and one might ask whether in fact models might exist where all the phases are naturally small, e.g. $O(10^{-2})$, thus resolving the EDM problem. We present now one such possibility.

Below the compactification scale M_c , one may analyse a model in terms of the supergravity functions of the chiral fields ϕ_α : the gauge kinetic function $f_{ij}(\phi_\alpha)$, the Kahler potential $K(\phi_\alpha, \phi_\alpha^\dagger)$ and the superpotential $W(\phi_\alpha)$. While the origin of supersymmetry breaking remains unknown, one may characterize it by assuming the existence of a hidden sector where some fields, e.g. moduli or dilaton, grow VEVs of Planck mass size:

$$x_i = \kappa < \Phi_i > = O(1). \quad (34)$$

Here $\kappa^{-1} = M_{Pl} = 2.4 \cdot 10^{18}$ GeV. We write $\{\Phi_\alpha\} = \{\Phi_i, \Phi_a\}$ where Φ_a are the physical sector fields and expand the Kahler potential in a power series of the physical fields:

$$K = \kappa^{-2} c^{(0)} + (c_{ab}^{(2)} \Phi_a \Phi_b + \frac{1}{M} c_{abc}^{(3)} \Phi_a \Phi_b \Phi_c + \dots) + (\tilde{c}_{ab}^{(2)} \Phi_a \Phi_b^\dagger + \frac{1}{M} \tilde{c}_{abc}^{(3)} \Phi_a^\dagger \Phi_b \Phi_c + \dots) \quad (35)$$

where M is a large mass. The $c^{(i)}, \tilde{c}^{(i)}$ are dimensionless functions of x_i and are assumed to be $O(1)$. The first parenthesis is holomorphic and hence can be transferred to the superpotential by a Kahler transformation:

$$W \rightarrow W + \kappa^2 W (c_{ab}^{(2)} \Phi_a \Phi_b + \frac{1}{M} c_{abc}^{(3)} \Phi_a \Phi_b \Phi_c + \dots) \quad (36)$$

The leading terms on the right arise when W is replaced by its VEV after SUSY breaking, ($\kappa^2 < W > \simeq m_{3/2}$) and one of the cubic terms (e.g. Φ_c) has a GUT scale VEV arising e.g. from the GUT group breaking to the Standard Model, $< \Phi_c > \simeq M_G$. This then gives rise to the μ term, $W \rightarrow W + \mu_{ab} \Phi_a \Phi_b$, where

$$\mu_{ab} = (c_{ab}^{(2)} + \frac{M_G}{M} c_{abc}^{(3)}) m_{3/2}. \quad (37)$$

If one assumes now that the renormalizable terms $c_{ab}^{(2)}$ in K is real, $c_{abc}^{(3)}$ is complex but with arbitrary size phase, μ^0 will grow a phase $\theta_{0\mu}$ of size M_G/M for $M \gg M_G$ without any fine tuning. For SUGRA models one expects $M = M_{Pl}$ and hence $\theta_{0\mu} \simeq O(10^{-2})$. Similar results can occur for the phases in the soft breaking

parameters and one might have a model where all phases are $O(10^{-2})$ naturally suppressing the EDMs without any fine tuning. For D-brane models considered here one expects $M = M_{\text{str}}$ and as discussed in Sec III, $M_{\text{str}} \cong 8 \times 10^{16}$ leading to phases of size $O(10^{-1})$. There is then a partial suppression of the EDMs leading perhaps to interesting predictions for the next round of EDM measurements for such models.

5 CONCLUSIONS

The very strong experimental constraints on the electron and neutron electric dipole moments put additional constraints on the parameter space of the SUSY models if the mass spectrum lies below ~ 1 TeV. We have studied this within the framework of models where the physics is determined at a high scale (e.g. GUT or Planck scale). For SUGRA GUT models the renormalization group equation naturally suppress α_t , the A_t phase at the electroweak scale, due to the nearness of the t-quark Landau pole and so the phase α_{0A} at M_G can be naturally large, even $\pi/2$, and still lead to acceptable EDMs. The possible cancelations of different parts of the EDM amplitudes does allow θ_B , the B phase at the electroweak scale, to be large, i.e. $O(10^{-1})$ when $\alpha_{0A} = O(1)$, but only for low $\tan\beta$ i.e. $\tan\beta \leq 3$. The combined conditions of the experimental EDM constraints and the requirement of radiative breaking of $SU(2) \times U(1)$ then leads to θ_{0B} to be $O(1)$ at the M_G and very tightly determined for $\tan\beta \gtrsim 3$. Thus there is a new fine tuning problem at M_G unless $\tan\beta$ is small. We note that LEP data already requires $\tan\beta > 2$, and the RUN II at the Tevatron will be able to probe higher $\tan\beta$ as it searches for the Higgs.

For a class of D brane models arising in Type IIB orientifolds, one can have the gaugino mass phases obey $\phi_1 = \phi_2 \neq \phi_3$ allowing θ_B to become larger due to additional cancelations between gluino and neutralino diagrams. However, the same fine tuning problem for θ_{0B} at M_G arises unless $\tan\beta$ is small. Further, one needs $\tan\beta \lesssim 5$ to get a significant overlap between the allowed d_e and d_n regions in parameter space when the ϕ_i are large.

The fact that the fine tuning problem of θ_{0B} appears to be endemic leads one to consider the possibility that all phases might naturally be small at M_G . A simple model showing this might arise where the phases $\phi_i = O(M_G/M)$ is discussed, where $M = M_{\text{Planck}}$ for SUGRA models and $M = M_{\text{string}}$ for D-brane models.

6 Acknowledgement

This work was supported in part by National Science Foundation Grant No. PHY-9722090.

References

1. P. G. Harris et al, *Phys. Rev. Lett.* **82**, 904 (1999).
2. E. Commins et al, *Phys. Rev. D* **50**, 2960 (1994); K. Abdullah et al, *Phys. Rev. Lett.* **65**, , (2340)1990.

3. J.-M. Gerard et al, *Nucl. Phys. B* **253**, 93 (1985); E. Franco and M. Mangano, *Phys. Lett. B* **135**, 445 (1984); A. Sanda, *Phys. Rev. D* **32**, 2992 (1985); M. Dugan, B. Grinstein and L. Hall, *Nucl. Phys. B* **255**, 413 (1985); W. Bernreuther and M. Suzuki, *Rev. Mod. Phys* **63**, 313 (1991).
4. P. Nath, *Phys. Rev. Lett.* **66**, , (2565)1991; Y. Kizhukuri and N. Oshimo, *Phys. Rev. D* **45**, 1806 (1992); *Phys. Rev. D* **46**, 3025 (1992); R. Garisto and J. Wells, *Phys. Rev. D* **55**, 611 (1997).
5. T. Ibrahim and P. Nath, *Phys. Lett. B* **418**, 98 (1998).
6. T. Ibrahim and P. Nath, *Phys. Rev. D* **57**, 478 (1998).
7. T. Ibrahim and P. Nath, *Phys. Rev. D* **58**, 111301 (1998).
8. T. Falk and K. Olive, *Phys. Lett. B* **439**, 71 (1998).
9. S. Barr and S. Khalil, hep-ph/9903425.
10. T. Falk, K. Olive, M. Pospelov and R. Roiban, hep-ph/9904393.
11. M. Brhlik, G. Good, and G. Kane, *Phys. Rev. D* **59**, 115004 (1999).
12. M. Brhlik, L. Everett, G. Kane and J. Lykken, hep-ph/9905215.
13. A. Bartl, T. Gajdosik, W. Porod, P. Stockinger and H. Stremnitzer, hep-ph/9903402.
14. S. Pokorski, J. Rosiek and C. A. Savoy, hep-ph/9906206.
15. E. Accomando, R. Arnowitt and B. Dutta, hep-ph/9907446.
16. E. Accomando, R. Arnowitt and B. Dutta, hep-ph/9909333 (to appear in *Phys. Rev. D*).
17. A. Chamseddine, R. Arnowitt and P. Nath, *Phys. Rev. Lett.* **49**, 970 (1982); for reviews see P. Nath, R. Arnowitt and A. Chamseddine, *Applied N=1 Supergravity*, World Scientific (1984); H. P. Nilles, *Phys. Rep. Phys. Rept.* **110**, 1 (1984).
18. D. Chang, W-Y. Keung and A. Pilaftsis, *Phys. Rev. Lett.* **82**, , (900)1999.
19. Dai et al, *Phys. Lett. B* **216**, 71 (1990).
20. R. Arnowitt, J. L. Lopez, D.V. Nanopoulos, *Phys. Rev. D* **42**, 2423 (1990); R. Arnowitt, M. Duff and K. Stelle, *Phys. Rev. D* **43**, 3085 (1991).
21. A. Manohar and H. Georgi, *Nucl. Phys. B* **234**, 189 (1984).
22. H. Leutwyler, *Phys. Lett. B* **374**, 163 (1996).
23. L.E. Ibanez and C. Lopez, *Nucl. Phys. B* **233**, 511 (1984); L.E. Ibanez, C. Lopez and C. Munoz, *Nucl. Phys. B* **256**, 218 (1985).
24. L. Ibanez, C. Munoz and S. Rigolin, *Nucl. Phys. B* **553**, 43 (1999).
25. G. Aldazabal, A. Font, L. Ibanez and G. Violero, *Nucl. Phys. B* **536**, 29 (1998).
26. A. Brignole, L. Ibanez, C. Munoz and C. Scheich, *Z. Phys* **C74**, 157 (1997).
27. A. Brignole, L. Ibanez and C. Munoz, *Nucl. Phys. B* **422**, 125 (1994) ; Erratum *ibid. Nucl. Phys. B* **436**, 747 (1995).

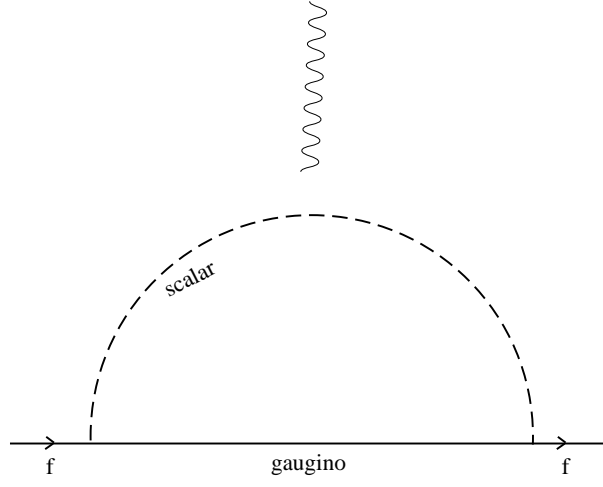


Figure 1. Diagrams contributing to d_f . For $f=q(l)$ the scalars are $\tilde{q}(\tilde{l})$ and gauginos are $\tilde{\chi}_i^0, \tilde{\chi}_i^\pm, \tilde{g}$ where $\tilde{\chi}_i^\pm, i=1,2$ are charginos and $\tilde{\chi}_i^0, i=1\dots4$ are neutralinos.

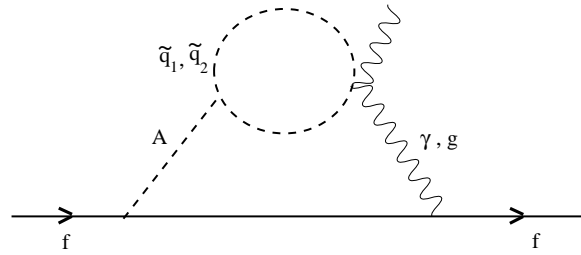
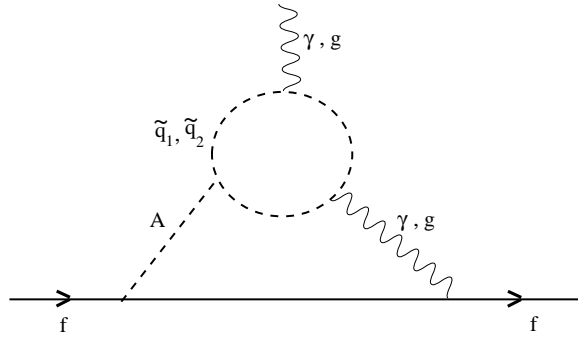


Figure 2. Two loop Barr-Zee diagrams where A is the CP odd Higgs and \tilde{q}_i are the mass diagonal squark states.

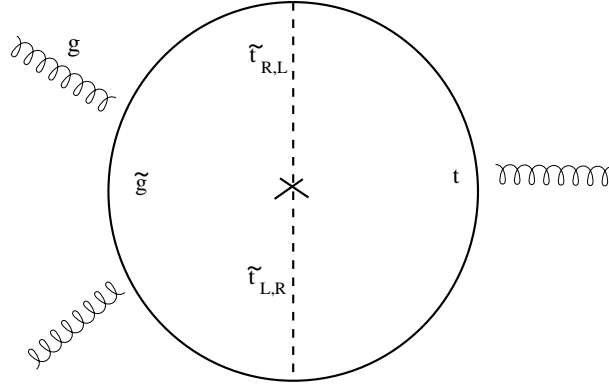


Figure 3. Two loop Weinberg type diagram.

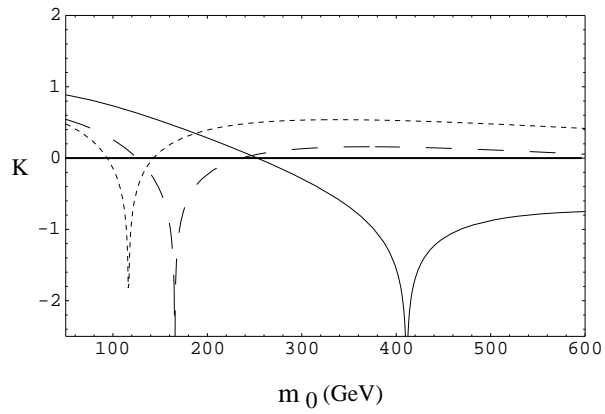


Figure 4. K vs m_0 for d_e (electron EDM) for $\tan\beta = 3$ (solid), 10 (dashed) and 20 (dotted) respectively for $m_{1/2} = 300$, $|A_0| = 300$ GeV, $\alpha_{0A} = \frac{\pi}{2}$, $\theta_B = 0.02$.

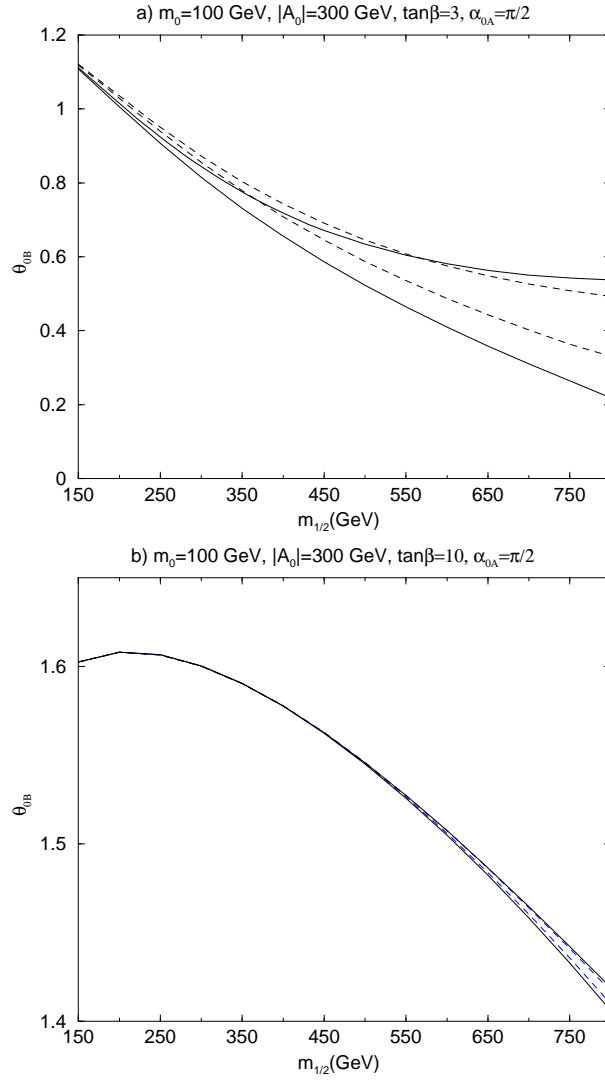


Figure 5. θ_{0B} vs $m_{1/2}$. Upper and lower lines are the allowed range so that $K \leq 0$. The solid lines are for d_n and the dotted lines are for d_e .

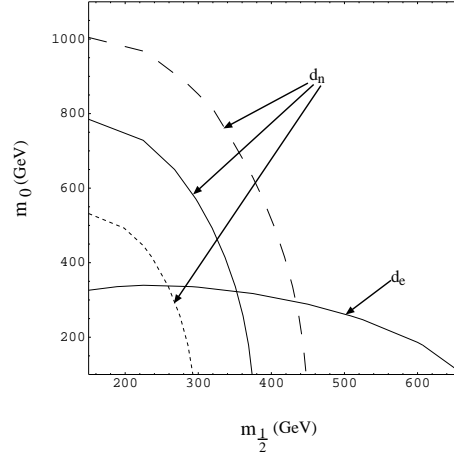


Figure 6. The $K=0$ contours are plotted as a function of m_0 and $m_{1/2}$. The dotted, solid and dashed lines are for m_d (1 GeV)=5, 8 and 12 MeV respectively. The other input parameters are $\alpha_{0A} = \frac{\pi}{2}$, $|A_0| = 300$ GeV $\theta_B=0$ and $\tan\beta=3$. Excluded regions are below d_e and to the left of d_n curves.

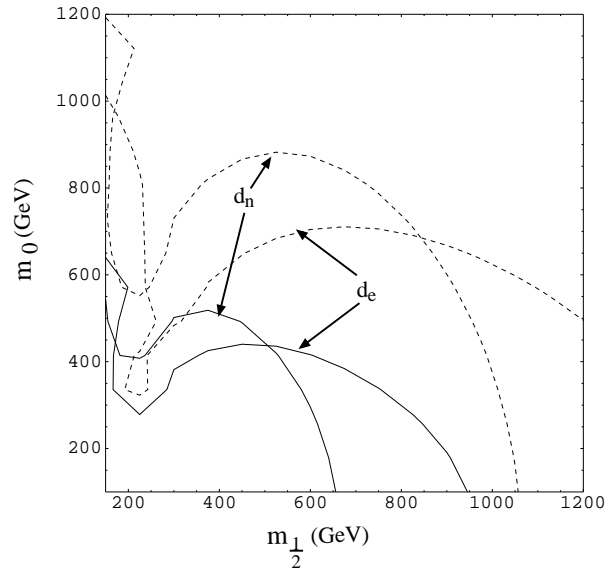


Figure 7. Allowed region in $m_0 - m_{1/2}$ plane for d_e and d_n . The other input parameters are $\alpha_{0A} = \frac{\pi}{2}$, $|A_0| = 300$ GeV, $\theta_B=0$ and $\tan\beta=20$. The solid lines are for $K=0$ and the dotted lines are for $K=-0.5$.

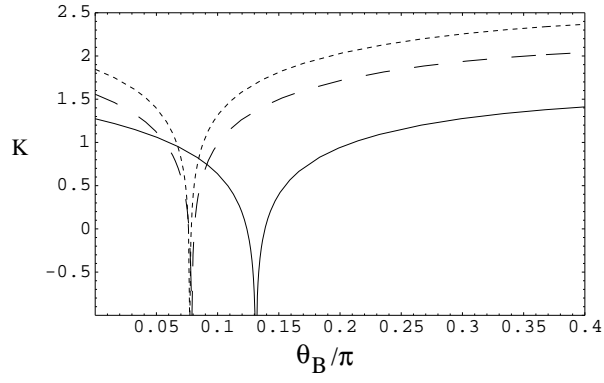


Figure 8. K vs. θ_B for d_e for $\phi_1=\phi_3=\pi+\alpha_{0A}=-1.25\pi$, $m_{3/2}=150$ GeV, $\theta_b=0.2$, $\Theta_1 = 0.85$, with $\tan\beta=2$ (solid), 5(dashed), 10(dotted).

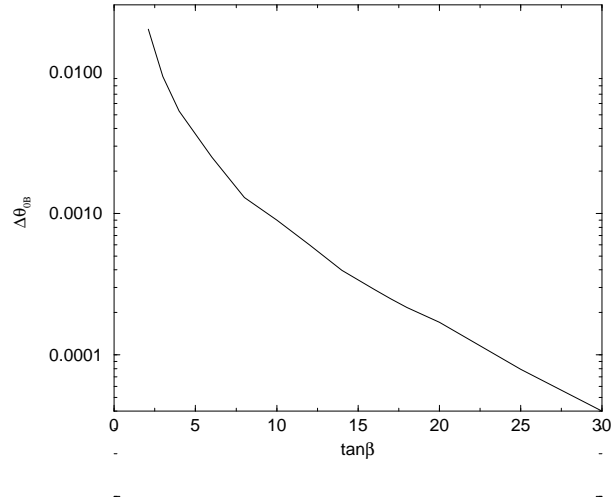


Figure 9. Values of $\Delta\theta_{0B}$ for d_e satisfying the EDM constraint as a function of $\tan\beta$. Parameters are as in Fig.8.

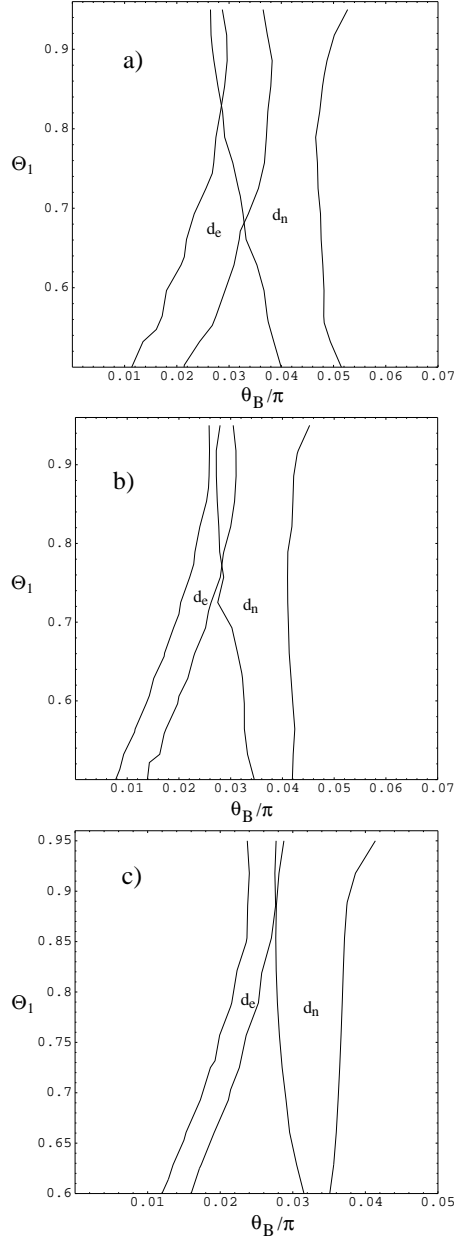


Figure 10. Allowed regions for d_e and d_n for $\theta_b=0.2$, $m_{3/2}=150$ GeV and $\phi_1=\phi_3=-1.90\pi$, for a) $\tan\beta=2$, b) $\tan\beta=3$ and c) $\tan\beta=5$.